A Physical Orbit for the High Proper Motion Binary HD 9939

Andrew F. Boden[1,2], Guillermo Torres[3], David W. Latham[3]

bode@ipac.caltech.edu

ABSTRACT

We report spectroscopic and interferometric observations of the high-proper motion double-lined binary system HD 9939, with an orbital period of approximately 25 days. By combining our radial-velocity and visibility measurements we estimate the system physical orbit and derive dynamical masses for the components of $M_A = 1.072 \pm 0.014$ $M_\odot$ and $M_B = 0.8383 \pm 0.0081$ $M_\odot$; fractional errors of 1.3% and 1.0%, respectively. We also determine a system distance of 42.23 ± 0.21 pc, corresponding to an orbital parallax of $\pi_{\rm orb} = 23.68 \pm 0.12$ mas. The system distance and the estimated brightness difference between the stars in V, H, and K yield component absolute magnitudes in these bands. By spectroscopic analysis and spectral energy distribution modeling we also estimate the component effective temperatures and luminosities as $T_{\rm eff}^A = 5050 \pm 100$ K and $T_{\rm eff}^B = 4950 \pm 200$ K and $L_A = 2.451 \pm 0.041$ $L_\odot$ and $L_B = 0.424 \pm 0.023$ $L_\odot$.

Both our spectral analysis and comparison with stellar models suggest that HD 9939 has elemental abundances near solar values. Further, comparison with stellar models suggests the HD 9939 primary has evolved off the main sequence and appears to be traversing the Hertzsprung gap as it approaches the red giant phase of its evolution. Our measurements of the primary properties provide new empirical constraints on stellar models during this particularly dynamic evolutionary phase. That HD 9939 is currently in a relatively short-lived evolutionary state allows us to estimate the system age as 9.12 ± 0.25 Gyr. In turn the age and abundance of the system place a potentially interesting, if anecdotal, constraint on star formation in the galactic disk.

Subject headings: binaries: spectroscopic — stars: fundamental parameters — stars: abundances — stars: individual (HD 9939)

[1]Michelson Science Center, California Institute of Technology, 770 South Wilson Ave., Pasadena CA 91125

[2]Department of Physics and Astronomy, Georgia State University, 29 Peachtree Center Ave., Science Annex, Suite 400, Atlanta GA 30303

[3]Harvard-Smithsonian Center for Astrophysics, 60 Garden St., Cambridge MA 02138

1. Introduction

Accurate determinations of the physical properties of stars in binary systems (mass, radius, luminosity, elemental abundance, etc.) provide for fundamental tests of models of stellar structure and stellar evolution. The most basic of those stellar properties is the mass, typically available only through analysis of dynamical interactions in general and binary systems in particular. Several dozen eclipsing binary systems have component mass and radius determinations that are accurate to 1–2% (e.g., Andersen 1991), and show that main-sequence models for stars with masses in the range from about 1 $M_{\odot}$ to 10 $M_{\odot}$ and elemental abundances near solar are in fairly good agreement with the observations. However, models for elemental compositions that are much different from solar are largely untested by observations due to a lack of suitable systems or a lack of accurate measurements. Consequently in 2000 we initiated a program to measure the properties of metal-poor stars in binary systems. The first results from that program were reported in Torres et al (2002, hereafter Paper 1). Here we follow Paper 1 with a report on our measurements of the high-proper motion binary system HD 9939.

HD 9939 (aka G34-39, HIP 7564, SAO 74830) is a relatively short-period (25 d) binary system. HD 9939 was identified as a high proper-motion object in the Luyten (Luyten 1980; Salim & Gould 2003, and references therein) and Lowell (Giclas, Burnham, & Thomas 1971, 1978) proper motion surveys. HD 9939 was included as part of the high-proper motion radial velocity survey program of Carney & Latham et al (see Carney & Latham 1987), where it was identified as a single (Latham et al. 1988) and eventually a double-lined spectroscopic binary (Goldberg et al. 2002, and references therein). (Separately HD 9939 was identified as a suspected binary system in the Mt. Wilson survey of Fouts and Sandage (Fouts 1987, and references therein)). The consensus spectral classification for the HD 9939 system is K0 IV by Bidelman (1985, based on observations by Kuiper) and Yoss (1961, responsible for the luminosity classification). Analysis of the spectra taken in the above-mentioned Carney & Latham project yielded an estimated HD 9939 system metallicity [Fe/H] = -0.51 dex (hence its inclusion in our program), and an estimated effective temperature of 4770 K. However both of these estimates were flagged as highly uncertain (Carney et al. 1994). Based on the double-lined orbit of Goldberg et al. (2002, hereafter G2002), Mazeh et al. (2003) included HD 9939 in a statistical study of mass ratios in binary systems.

HD 9939 was identified as a candidate for our program on metal-poor systems in 2000, and observed with the Palomar Testbed Interferometer (PTI) and Harvard-Smithsonian Center for Astrophysics (CfA) telescopes. Herein we report the physical orbit estimation for HD 9939 based on these observations, and the analysis of the system components based on the physical orbit.

2. Observations

2.1. Spectroscopy

HD 9939 was observed at the CfA with an echelle spectrograph on the 1.5-m Wyeth reflector at the Oak Ridge Observatory (eastern Massachusetts), and occasionally also with a nearly identical instrument on the 1.5-m Tillinghast reflector at the F. L. Whipple Observatory (Arizona). A single echelle order was recorded using intensified photon-counting Reticon detectors, spanning about 45 Å at a central wavelength of 5188.5 Å, which includes the Mg I b triplet. The resolving power of these instruments is $\lambda/\Delta\lambda \approx 35{,}000$, and the signal-to-noise (S/N) ratios achieved range from 11 to about 47 per resolution element of 8.5 km s^{-1}. A total of 62 spectra were obtained between 6 September 1982 and 4 February 2002, spanning 19.4 years and 281 system periods, with many spectra taken relatively recently as HD 9939 was included in our joint program.

Radial velocities (RVs) were determined from the spectra with the two-dimensional cross-correlation algorithm TODCOR (Zucker & Mazeh 1994), which uses two templates, matched to each component of the binary. The templates were selected from an extensive library of calculated spectra based on model atmospheres by R. L. Kurucz[1], computed for us by Jon Morse (see also Nordström et al. 1994; Latham et al. 2002). These calculated spectra are available for a wide range of effective temperatures ($T_{\rm eff}$), rotational velocities ($v_{\rm rot}$), surface gravities ($\log g$), and metallicities. The optimum template for each star was determined from grids of cross-correlations over broad ranges in temperature and rotational velocity (since these are the parameters that affect the radial velocities the most), seeking to maximize the average correlation weighted by the strength of each exposure. Surface gravities of $\log g = 4.0$ for the primary and $\log g = 4.5$ for the secondary were adopted from the results of §4. The grids of correlations were repeated for a range of metallicities, and we found that our spectra have a strong preference for a composition near solar, as opposed to the more negative but uncertain value of [m/H] = −0.51 reported by Carney et al. (1994). Consequently we adopted the solar value for determining the RVs. The temperature estimates from our spectra for this metallicity are $T_{\rm eff}^A = 5050 \pm 100$ K and $T_{\rm eff}^B = 4950 \pm 200$ K for the primary and secondary, respectively. The rotational broadening of the stars was found to be negligible. The light ratio inferred from these spectra at the mean wavelength of our observations is $\ell_B/\ell_A = 0.16 \pm 0.03$.

Following our procedures in Paper 1 we tested our velocities for systematic effects by means of numerical simulations. The corrections were found to be small (typically well under

[1]Available at `http://cfaku5.cfa.harvard.edu`.

1 km s^{-1}), but were applied nevertheless for consistency. The final velocities including these corrections are presented in Table 1. These measurements, and the orbital solutions derived from them below, supersede those obtained by G2002 that were based on a subset of the present spectra.

2.2. Interferometry

As in Paper I, the interferometric observable used for these measurements is the fringe contrast or *visibility* (squared) of an observed brightness distribution on the sky. PTI was used to make the interferometric measurements presented here; PTI is a long-baseline H (1.6μm) and K-band (2.2μm) interferometer located at Palomar Observatory, and described in detail elsewhere (Colavita et al. 1999). The analysis of such data on a binary system is discussed in detail in previous work (e.g. Boden et al. 2000) and elsewhere (e.g. Hummel et al. 1998) and is not repeated here.

HD 9939 was observed in conjunction with objects in our calibrator list by PTI in K band ($\lambda \sim 2.2\mu$m) on 91 nights between 9 August 2000 and 13 December 2004, a dataset spanning roughly 4.3 years and 62 orbital periods. Additionally, HD 9939 was observed by PTI in H band ($\lambda \sim 1.6\mu$m) on six nights between 15 September 2000 and 18 August 2002, spanning roughly two years and 28 system periods. On each night HD 9939 and calibration objects were typically observed repeatedly, and each observation, or scan, was approximately 130 sec long. For each scan we computed a mean V^2 value from the scan data, and the error in the V^2 estimate from the rms internal scatter (Colavita 1999; Boden et al. 1998). HD 9939 was observed in combination with one or more calibration sources within $\sim 10^\circ$ on the sky. Here we have used two stars as calibration objects: HD 7034 (putative F0 V), HD 7964 (putative A3 V); Table 2 lists the relevant physical parameters for the calibration objects. Calibrating our interferometric data using the these objects results in 542 K and 60 H visibility scans on HD 9939. The calibrated V^2 data on HD 9939 are summarized in Table 3.

3. Orbit Determination

As in Paper 1, we have estimated the HD 9939 orbit based separately on the CfA spectroscopy, the PTI visibilities, and jointly with these two datasets.

Figure 1 depicts the relative visual orbit of the HD 9939 system, with the primary component rendered at the origin, and the secondary component rendered at periastron. We

have indicated the phase coverage of our V^2 data on the relative orbit with heavy lines; our data sample essentially all phases of the orbit, leading to a reliable orbit determination. The size of the HD 9939 components are estimated (see discussion in §4) and rendered to scale.

V^2 observations are subject to a point-symmetric inversion degeneracy (a scene and its mirror inverse produce the same V^2), so astrometric orbits determined with such data have a modulo 180° uncertainty in the apparent orientation on the sky and longitude of the ascending node (Ω) (e.g. Boden et al. 2000, 2005). In the case of HD 9939 there is a significant brightness ratio between the components, so we modeled archival Hipparcos intermediate astrometric data constrained by the high-precision orbital parameters determined here (Table 4) to determine the proper orientation/Ω value. The small angular scale orbit is marginally resolved in the Hipparcos data. However fixing all parameters except the photocentric semi-major axis and Ω indicates the quadrant value of Ω as given in Table 4 and as rendered in Figure 1 (i.e. with the secondary North-East of the primary at periastron). Therefore we believe the proper orientation of the HD 9939 orbit is as rendered, and Ω is uniquely determined as given in Table 4.

Figure 2 depicts the phase-folded radial velocity orbit of HD 9939. The top frame gives the RV orbit curves and the measured radial velocities from Table 1. The bottom frame gives the residuals between our RV data and the orbit model (data - model). Our solution is in good agreement with the G2002 double-lined solution derived from many of the same spectra.

Table 4 summarizes orbit models for HD 9939, including the model from G2002, and individual and joint fits to our visibility and radial velocity datasets. All solutions have component diameters constrained as noted above. All orbit parameters are listed with total one-sigma errors, including contributions from statistical (measurement uncertainty) and systematic error sources. In our analysis the dominant forms of systematic error are: (1) uncertainties in the calibrator angular diameters (Table 2); (2) uncertainty in the center-band operating wavelength ($\lambda_0 \approx 2.2$ μm), taken to be 10 nm (∼0.5%); (3) the geometrical uncertainty in our interferometric baseline ($< 0.01\%$); and (4) uncertainties in ancillary parameters constrained in our orbit fitting procedure (i.e. the angular diameters in all solutions involving interferometry data).

4. Physical properties of HD 9939

The orbital parameters from Table 4 allow us to compute many of the physical properties of the HD 9939 system and its components. Physical parameters derived from our HD 9939

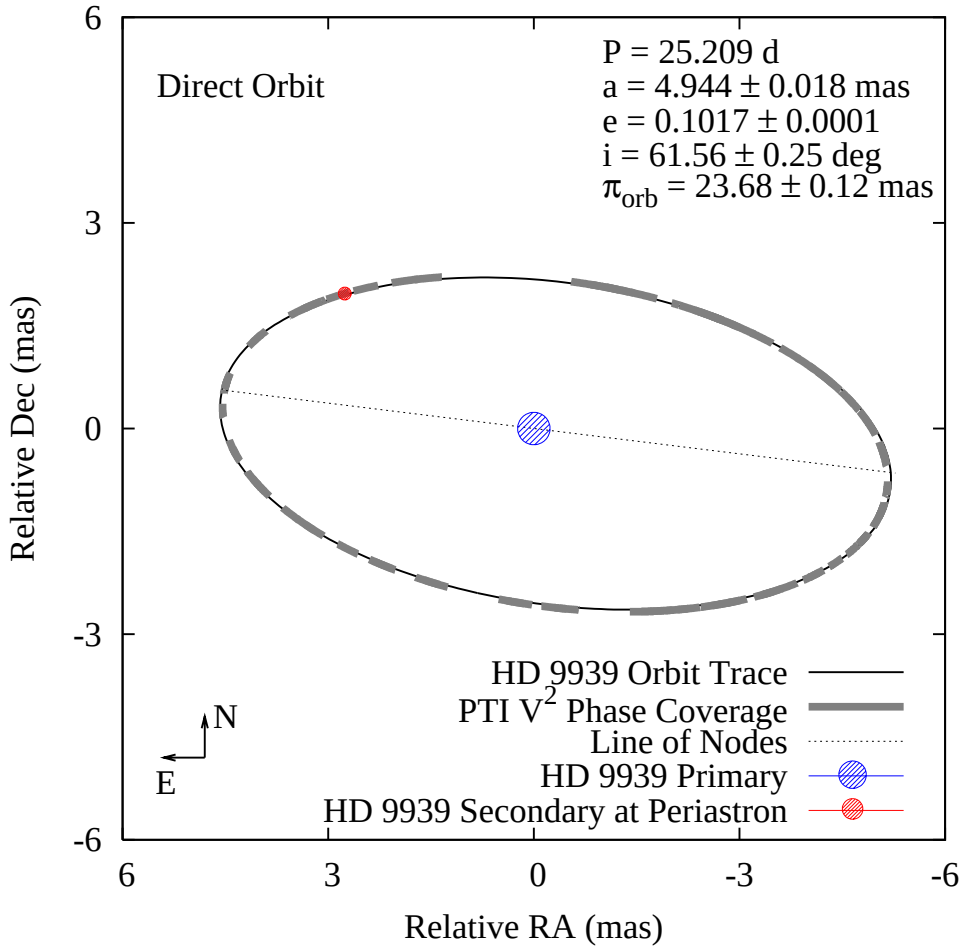

Fig. 1.— Visual Orbit of HD 9939. The relative visual orbit model of HD 9939 is shown, with the primary and secondary objects rendered at T_0 (periastron). The heavy lines along the relative orbit indicate areas where we have phase coverage in our K-band PTI data (they are not separation vector estimates); our data sample essentially all phases of the orbit well, leading to a reliable orbit determination. Component diameter values are estimated (see §4) and rendered to scale.

Table 2. PTI HD 9939 V^2 Calibration Objects in our Analysis. The relevant parameters for our two calibration objects are summarized. The apparent diameter values are determined from spectral energy distribution modeling based on archival broad-band photometry, spectral energy distribution templates from Pickles (1998), and visibility measurements with PTI.

Object Name	Spectral Type	Star Magnitude	Separation from HD 9939	Adopted Model Diameter (mas)
HD 7034	F0 V	5.2 V/4.4 K	8.5°	0.51 ± 0.02
HD 7964	A3 V	4.7 V/4.5 K	4.5°	0.42 ± 0.04

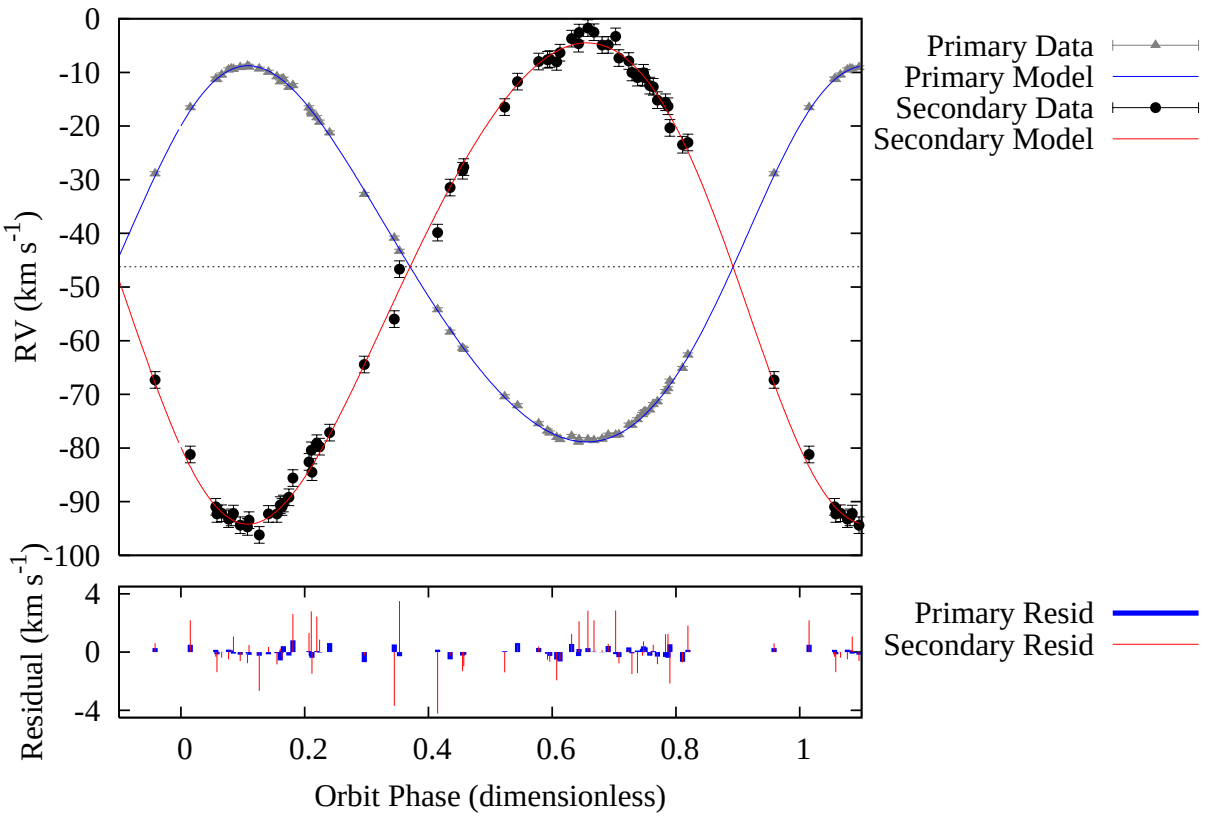

Fig. 2.— Radial Velocity Orbit of HD 9939. A phase-folded plot of our radial velocity data and RV predictions from our Full-Fit solution (Table 4). The lower frame gives RV residuals to the model fit.

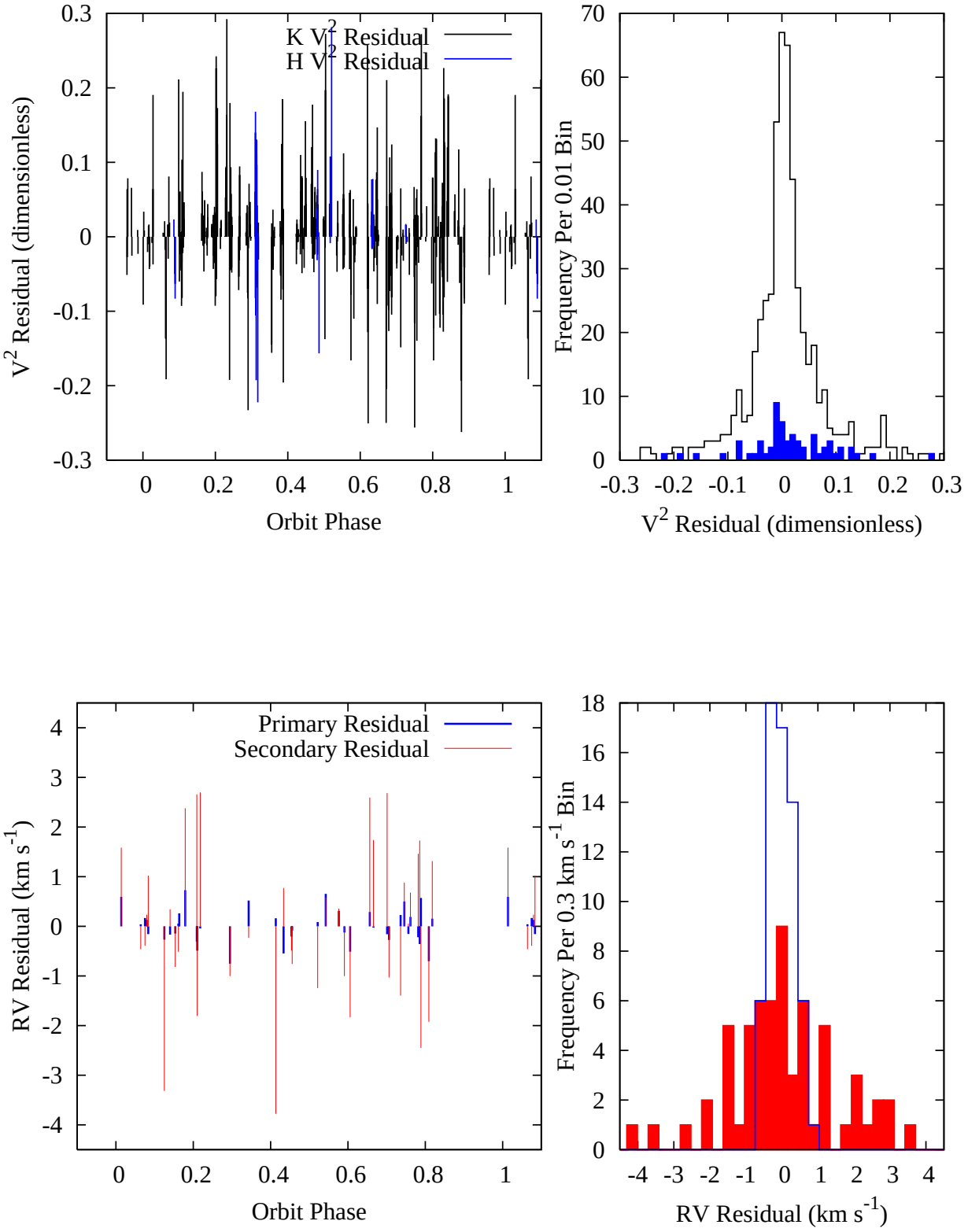

Fig. 3.— Orbit Modeling Residuals for HD 9939. Phase-folded residual plots and residual histograms are given for the V^2 (top) and RV (bottom) datasets relative to our Full-Fit solution (Table 4).

Table 4. Orbital Parameters for HD 9939. Summarized here are the apparent orbital parameters for the HD 9939 system as determined by G2002 and present results. We give three separate fits to our data: K V^2 only, RV only, and integrated ("Full Fit"). Ω is reported in a Position Angle convention.

Orbital Parameter	G2002	PTI & CfA		
		K V^2 Only	RV Only	Full-Fit
Period (d)	25.2125	25.20942	25.208918	25.208958
	± 0.018	± 4.5×10^{-4}	± 8.5×10^{-5}	± 7.2×10^{-5}
T_0 (MJD)	46039.24	51786.63	51786.368	51786.408
	± 0.22	± 0.13	± 0.083	± 0.063
e	0.1045	0.1006	0.1023	0.10166
	± 0.0046	± 0.0012	± 0.0019	± 0.00097
K_1 (km s^{-1})	35.17 ± 0.17		34.965 ± 0.056	34.952 ± 0.055
K_2 (km s^{-1})	44.89 ± 0.80		44.69 ± 0.24	44.68 ± 0.24
γ (km s^{-1})	-45.92 ± 0.12		-46.148 ± 0.054	-46.157 ± 0.049
ω_1 (deg)	312.7 ± 3.0	315.8 ± 1.6	312.6 ± 1.2	313.07 ± 0.88
Ω (deg)		262.55 ± 0.26		262.29 ± 0.20
i (deg)		61.06 ± 0.31		61.56 ± 0.25
a (mas)		4.937 ± 0.020		4.944 ± 0.018
$\Delta K_{\rm CIT}$ (mag)		1.983 ± 0.067		1.983 ± 0.067
$\Delta H_{\rm CIT}$ (mag)				2.00 ± 0.14
ΔV (mag)	2.06		1.990 ± 0.176	1.990 ± 0.176
χ^2/DOF		*1.0*	*1.0*	*1.0*
$\overline{\lvert R_{V^2}\rvert}/\sigma_{V^2}$		0.059/0.11		0.057/0.11
$\overline{\lvert R_{RV}\rvert}/\sigma_{RV}$ (km s^{-1})			0.70/1.1	0.81/1.18

"Full-Fit" integrated visual/spectroscopic orbit and spectral energy distribution modeling are summarized in Table 5. Notable among these is the high-precision determination of the component masses for the system; we estimate the masses of the primary and secondary components as 1.072 ± 0.014 and 0.8383 ± 0.0081 $M_\odot$, respectively. The relative errors in the primary and secondary component mass estimates are 1.3% and 0.97% respectively.

The Hipparcos catalog lists the parallax of HD 9939 as 23.80 ± 0.86 mas (ESA 1997). The distance determination to HD 9939 based on our orbital solution is 42.23 ± 0.21 pc, corresponding to an orbital parallax of 23.68 ± 0.12 mas, consistent with the Hipparcos result at 0.5% and 0.1-sigma.

At the distance of HD 9939 neither of the system components are significantly resolved by the PTI H or K-band fringe spacings, and we must resort to spectral energy distribution (SED) modeling to estimate the component diameters. As input to the SED modeling we have used archival photometry and the estimated component flux ratios in the spectroscopic and visibility data (Table 4). To this data we have fit a two-component model with solar abundance SED templates from Pickles (1998). We find a best-fit solution with Pickles templates matching spectral types K1 IV and K0 V, in good agreement with the system spectral classification. This SED model is depicted in Figure 4. Integrating the model component SEDs we estimate bolometric fluxes of $(4.418 \pm 0.059) \times 10^{-8}$ and $(7.65 \pm 0.40) \times 10^{-9}$ erg cm^{-2} s^{-1} for the HD 9939 primary and secondary components respectively. When combined with our component model effective temperatures (§2.1) we estimate apparent angular diameters of 0.451 ± 0.018 and 0.196 ± 0.017 mas for the primary and secondary components respectively. At the distance of HD 9939 the bolometric fluxes imply luminosities of 2.451 ± 0.041 and 0.424 ± 0.023 $L_\odot$, and physical radii of 2.048 ± 0.081 and 0.887 ± 0.071 $R_\odot$ for the primary and secondary components respectively.

5. Comparison with Stellar Evolution Models

With our estimates of the component masses, absolute magnitudes, color indices, and effective temperatures derived from our measurements and orbital solution (Table 5), we proceed in this section to examine the physical state of the HD 9939 components in the context of recent stellar evolution models from the Yonsei-Yale (Y^2) collaboration (Yi et al. 2001; Demarque et al. 2004).

Figure 5 gives coarse comparisons between the inferred properties of the HD 9939 components and Y^2 evolutionary tracks computed for a range of elemental abundances in empirical and theoretical color-magnitude spaces. The left column of Figure 5 shows comparisons

Table 5. Physical Parameters for HD 9939. Summarized here are the physical parameters for the HD 9939 system as derived primarily from the "Full-Fit" solution orbital parameters in Table 4. Archival system photometry is from Mermilliod & Mermilliod (1994) and Skrutskie et al. (1997).

Physical Parameter	Primary (A) Component	Secondary (B) Component
a (10^{-2} AU)	9.163 ± 0.026	11.712 ± 0.062
Mass ($M_\odot$)	1.072 ± 0.014	0.8383 ± 0.0081
Sp Type	K0 IV	
System Distance (pc)	42.23 ± 0.21	
π_{orb} (mas)	23.68 ± 0.12	
Bolometric Flux (10^{-9} erg cm^{-2} s^{-1})	44.18 ± 0.59	7.65 ± 0.40
T_{eff} (K)	5050 ± 100	4950 ± 200
Model Diameter (mas)	0.451 ± 0.018	0.196 ± 0.017
Luminosity ($L_\odot$)	2.451 ± 0.041	0.424 ± 0.023
Radius ($R_\odot$)	2.048 ± 0.081	0.887 ± 0.071
log g	3.845 ± 0.035	4.465 ± 0.070
$M_{K-\mathrm{CIT}}$ (mag)	1.896 ± 0.022	3.881 ± 0.062
$M_{H-\mathrm{CIT}}$ (mag)	2.027 ± 0.023	4.027 ± 0.12
M_V (mag)	4.003 ± 0.033	5.99 ± 0.15
V-K (mag)	2.080 ± 0.037	2.09 ± 0.16

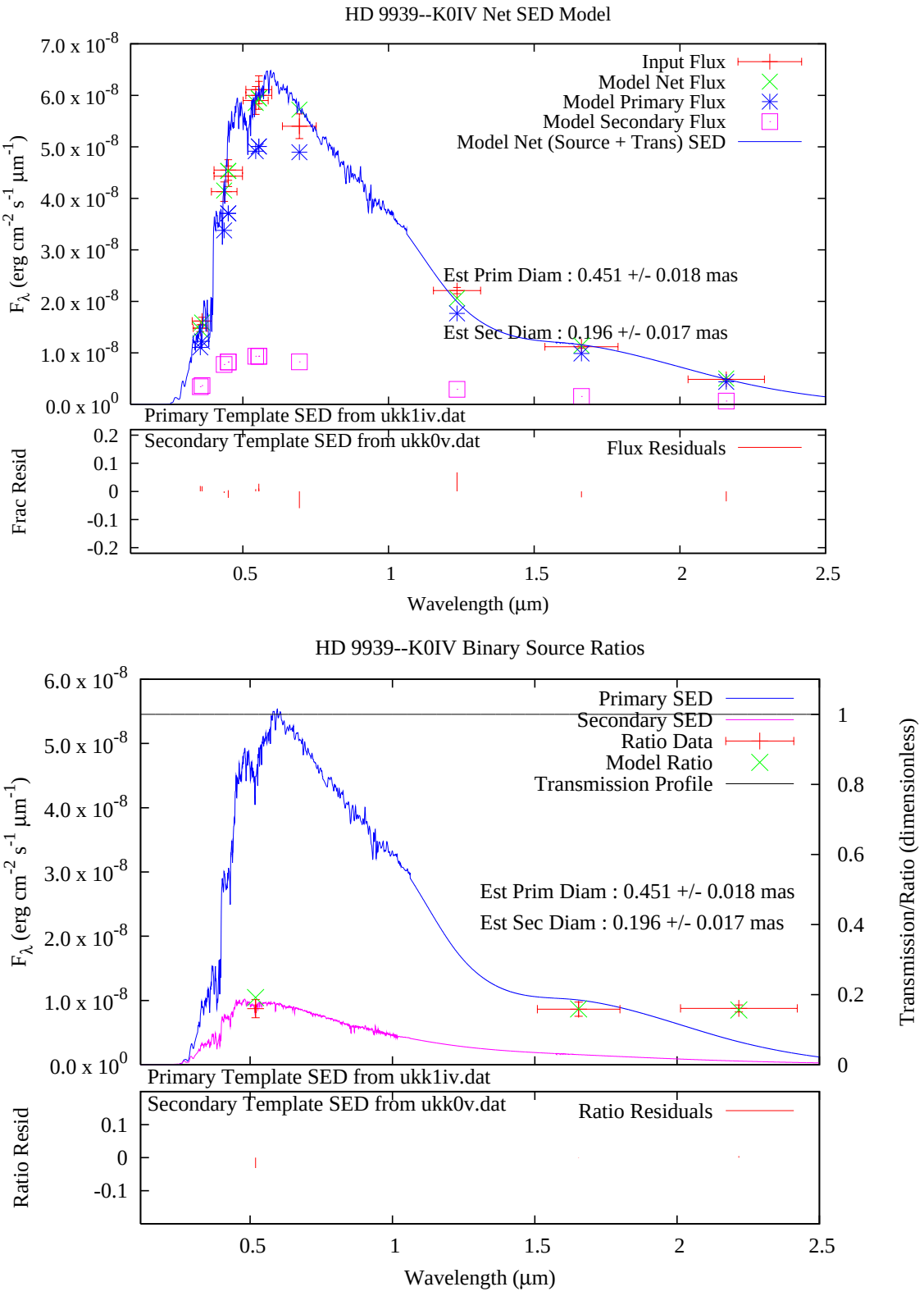

Fig. 4.— Spectral Energy Distribution Model for HD 9939. Here SED templates from Pickles (1998) have been simultaneously fit to archival photometry (top) and flux ratio estimates (bottom) from our visibility and spectroscopic measurements (Table 4).

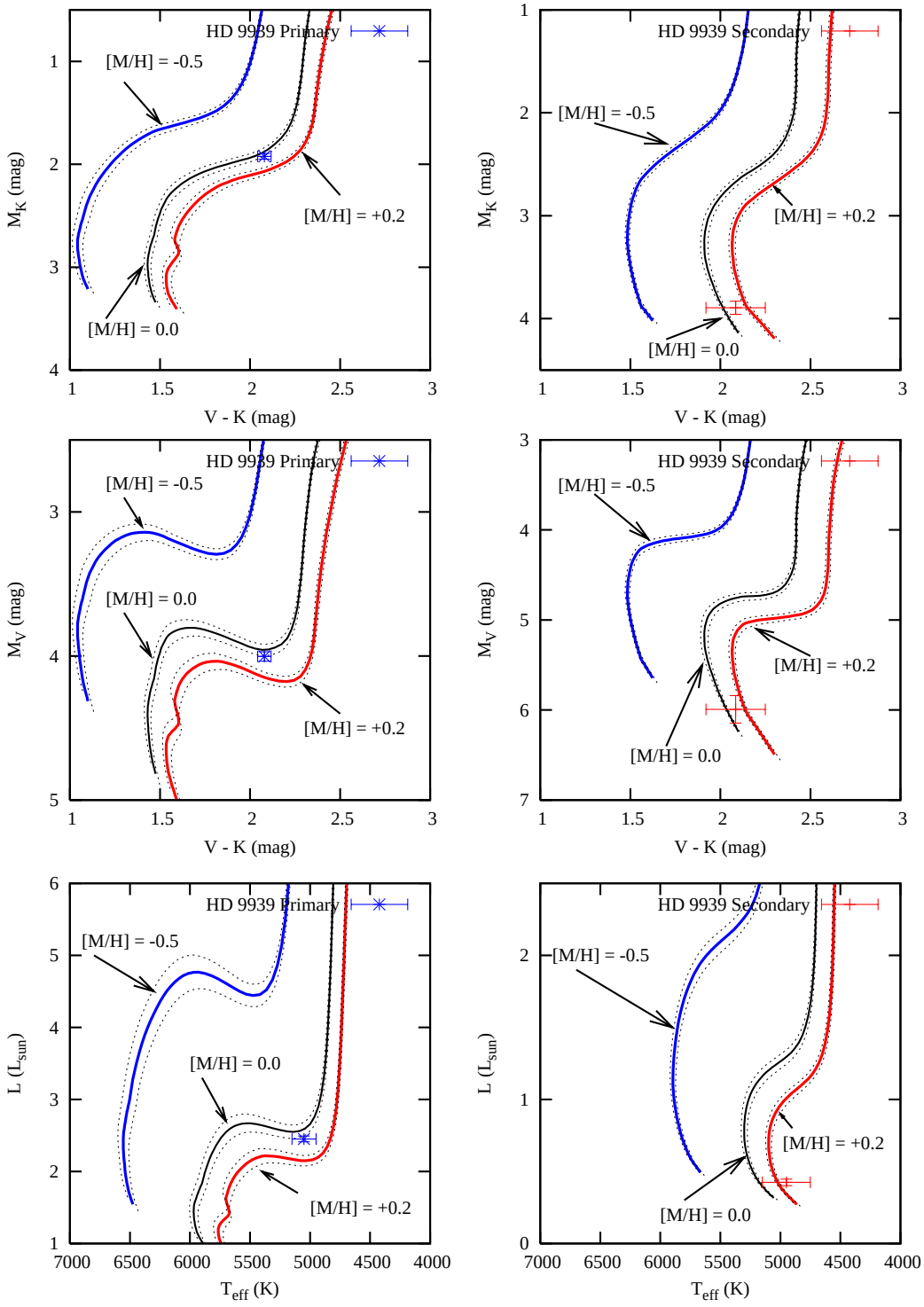

Fig. 5.— Gross HD 9939 Component/Y^2 Model Comparisons in Color-Magnitude Spaces. Positions of the HD 9939 components (primary – left column, secondary – right column) are given in empirical and theoretical color-magnitude spaces. Y^2 evolutionary tracks are given corresponding to the component dynamical mass estimates (with one-sigma errors, Table 5) for abundance values of [M/H] = -0.5, 0, and +0.2. Clearly the estimated component parameters are better matches for a roughly solar abundance than either sub- or super-solar abundances.

between observed properties for the HD 9939 primary and evolutionary tracks computed for the primary dynamical mass (with one-sigma errors; Table 5) and [M/H] abundances of -0.5, 0.0, and +0.2 dex. Similarly, the right column gives the corresponding comparisons for the HD 9939 secondary. Comparisons with the Y^2 models reinforce the conclusion from our spectroscopic analysis (§2.1); the elemental abundance for the HD 9939 system is not sub-solar as had been thought (e.g. Carney et al. 1994), but instead is near the solar value.

With the realization that the HD 9939 abundance is approximately solar, we have used the Y^2 models to evaluate the best match in elemental abundance for the inferred component parameters. Figure 6 shows the results of that process. The left column of Figure 6 shows the results of an abundance optimization using all the depicted component parameters ($V-K$, M_K, M_V, T_{eff}, L). We find excellent agreement for all these parameters with an abundance of [M/H] = +0.05. However if we ignore the inferred T_{eff} and luminosity, we find a slightly better match for the remaining component parameters at an [M/H] = +0.09 (Figure 6, right column). The Y^2 models suggest an elemental abundance for HD 9939 of [M/H] = 0.05 ± 0.05 dex.

Figure 6 indicates that the HD 9939 secondary is on the main sequence, while the HD 9939 primary is apparently in the Hertzsprung gap, a period of rapid evolution between the end of the main sequence and the bottom of the red giant branch. While it is a priori unlikely to find a star in this location in the HR-diagram (a star with the mass and abundance of the HD 9939 primary spends only approximately 450 Myrs in this phase, roughly 5% of the present system age), there is no apparent alternative to this conclusion. This makes the HD 9939 primary a potentially important test of stellar models.

Finally, Figure 6 indicates times along the evolutionary tracks consistent with the one-sigma excursions in the measured component parameters. As the HD 9939 secondary's radiative properties are relatively poorly measured and its position on the main sequence (where evolution is relatively slow), a large range of ages (roughly 7 – 10 Gyrs) is consistent with the inferred parameters. However, the better determined radiative properties of the HD 9939 primary, coupled with the star's rapid evolution in the Hertsprung gap results in a smaller viable age range. For instance, at a fixed [M/H] of +0.05, the range of ages implied by the Y^2 track is only 9.09 – 9.16 Gyrs (the corresponding range for [M/H] of +0.09 is 9.29 – 9.33 Gyrs). As the system abundance is uncertain at approximately 0.05 dex, we estimate the HD 9939 primary age at 9.12 ± 0.25 Gyrs (making no allowance for possible systematic errors in the Y^2 models.) This estimate is completely consistent with the large secondary range, so we adopt the primary age estimate for the HD 9939 system. Our system age estimate should be more reliable than the 4.6 Gyr value given by Wright et al. (2004) based on measurements of chromospheric Ca II H & K activity; the Wright et al. (2004)

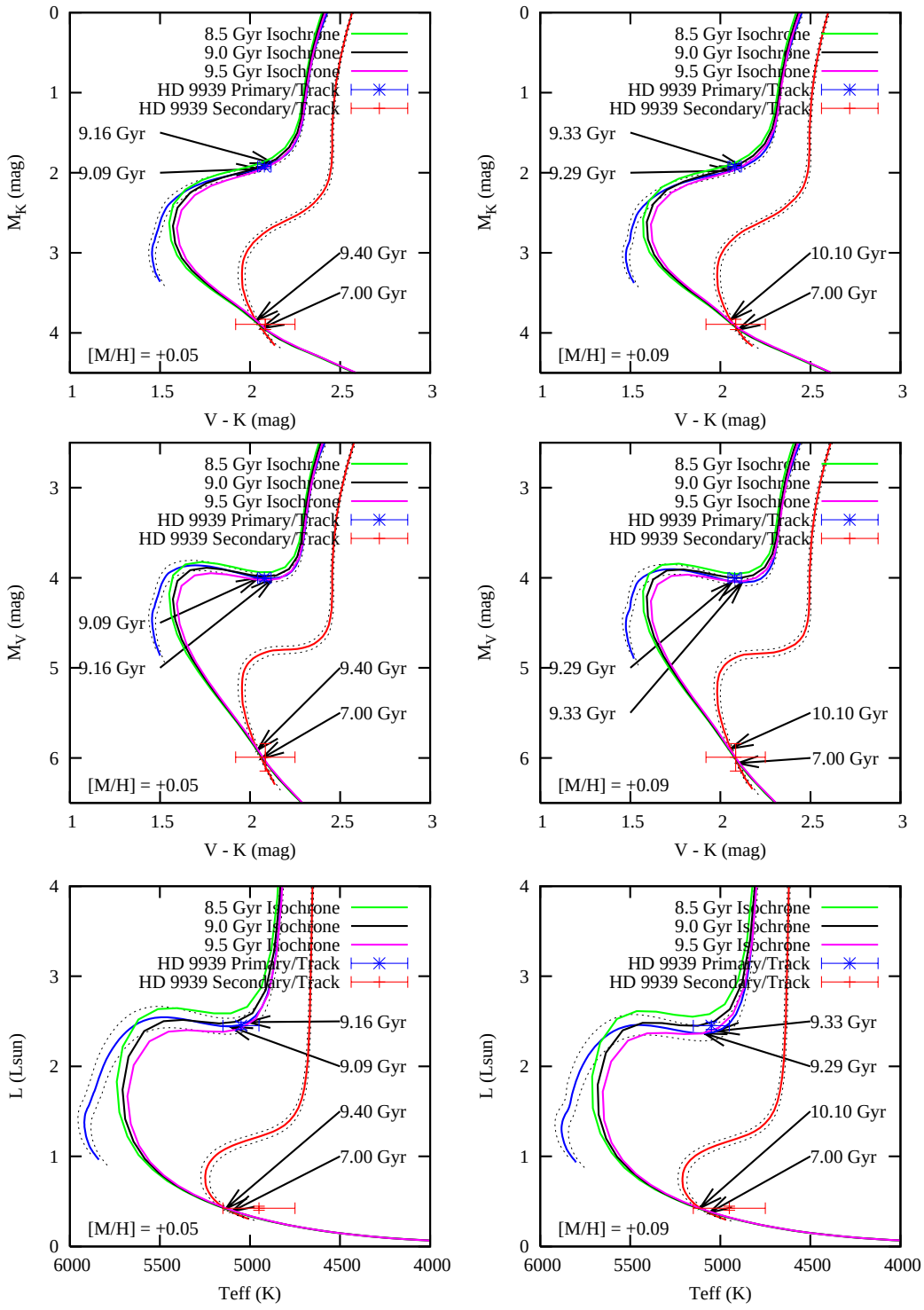

Fig. 6.— Detailed HD 9939 Component/Y^2 Model Comparisons in Observational and Theoretical Color-Magnitude Spaces. Best-fit Y^2 evolutionary tracks and isochrones are given for abundances with ([M/H] = +0.05, left column) and without ([M/H] = +0.09, right column) inclusion of theory-space parameters in the comparisons. The range of track-implied ages for the individual components are marked along the tracks. The primary luminosity estimate favors the [M/H] = +0.05/9.1 Gyr hypothesis.

estimate for HD 9939 ignored both the binarity of the system and the subgiant nature of the primary[2].

6. Discussion

The consensus from our spectroscopic data and component parameter comparisons with the Y^2 models makes it clear that the abundance of HD 9939 is approximately solar. Figure 6 shows that the Y^2 models do an excellent job of predicting the parameters for the HD 9939 components, and suggest that the elemental abundance for HD 9939 is [M/H] = +0.05 ± 0.05. These model comparisons further make it clear that the HD 9939 primary is currently traversing the Hertzsprung gap, and as such it is currently in a rapid phase of its evolution. Our determinations of dynamical mass, luminosity, and abundance for the primary make it an important empirical constraint for stars in this phase of evolution. Earlier provisional assessments of sub-solar abundance for HD 9939 were apparently biased by the unmodeled subgiant nature of the primary[3].

The combination of the HD 9939 primary's evolutionary state and the precision of our dynamical mass and radiometric parameter determinations allow us to estimate the HD 9939 age with surprising precision at 9.12 ± 0.25 Gyrs. This age is qualitatively consistent with the high space motion of the HD 9939 system at 82.51 ± 0.91 km s^{-1} with respect to the LSR (U = 80.32 ± 0.41 km s^{-1}, V = -18.13 ± 0.60 km s^{-1}, W = -5.34 ± 0.55 km s^{-1}, using conventions from Johnson & Soderblom 1987).

Kinematically it is unclear whether HD 9939 is a member of the galactic thin disk or galactic thick disk; its position in a kinematic Toomre diagram (e.g. Fuhrmann 2002; Venn et al. 2004) is shared between these two populations (however Nordström et al. 2004, discuss pitfalls of such kinematic classification). Based on the velocity ellipsoid models of Venn et al. (2004) we compute a relative thick/thin disk probability of 65%/35%. If HD 9939 is a thick disk member then it would be among the youngest and most metal-rich members of that population. Independent of population interpretation, HD 9939 is notable in abundance for a star its age. For instance, the age-metallicity studies of Rocha-Pinto et al. (2000) found no stars the age and metallicity of HD 9939 in their sample. However, prior (notably Edvardsson et al. 1993) and subsequent (e.g. Feltzing et al. 2001; Nordström et al. 2004) studies have found examples of stars with similar ages and metallicities as HD 9939. Narrowly

[2]Wright 2006, private communication

[3]Carney 2005, private communication

the parameters of the HD 9939 system clearly support the tenets that old, metal-rich stars do exist, and there is large metallicity dispersion at all stellar ages.

Old, metal-rich stars suggest that portions of the galactic disk reached significant metallicity early in its evolution (e.g. see Feltzing et al. 2001). HD 9939's well-determined age and abundance place potentially interesting constraints on such formation scenarios. Based on an epicycle approximation to HD 9939's galactic orbit (Binney & Tremaine 1987; Makarov et al. 2004), the velocity of HD 9939 implies minimum and maximum galactic radii of roughly 5.0 and 9.5 kpc respectively, and a mean galactic radius of 7.3 kpc (with $R_0 \sim 8.0$ kpc). Taking the mean radius as the likely formation radius for HD 9939 (following argument from Rocha-Pinto et al. 2004), that roughly solar-abundance stars were forming 9 Gyrs ago 7.3 kpc from in the galactic center is remarkable.

The authors thank the anonomous referee for thoughtful contributions to the presentation of the results presented here. We also thank Bruce Carney and Jason Wright for candid and cordial discussions on various technical aspects of their prior work on the HD 9993 system. Work done with the Palomar Testbed Interferometer was performed at the Michelson Science Center, California Institute of Technology under contract with the National Aeronautics and Space Administration. Interferometer data were obtained at Palomar Observatory using the NASA Palomar Testbed Interferometer, supported by NASA contracts to the Jet Propulsion Laboratory. Science operations with PTI are conducted through the efforts of the PTI Collaboration (http://huey.jpl.nasa.gov/palomar/ptimembers.html), and we acknowledge the invaluable contributions of our PTI colleagues. We particularly thank Kevin Rykoski for his professional operation of PTI. We thank Joe Caruso, Bob Davis, Robert Stefanik, and Joe Zajac for obtaining many of the spectroscopic observations used here. Thanks also to Valeri Makarov for valuable discussions concerning galactic orbits. GT acknowledges partial support from NASA's MASSIF SIM Key Project (BLF57-04) and NSF grant AST-0406183. This research has made use of services of the MSC at the California Institute of Technology; the SIMBAD database, operated at CDS, Strasbourg, France; of NASA's Astrophysics Data System Abstract Service; and of data products from the Two Micron All Sky Survey, which is a joint project of the University of Massachusetts and the Infrared Processing and Analysis Center, funded by NASA and the National Science Foundation.

REFERENCES

Andersen, J. 1991, A&A Rev. 3, 91.

Bidelman, W. 1985, ApJS 59, 197.

Binney, J. & Tremaine, S. 1987, "Galactic Dynamics", Princeton.

Boden, A., Colavita, M., van Belle, G., & Shao, M. 1998, Proc. SPIE 3350, 872.

Boden, A., Creech-Eakman, M., & Queloz, D. 2000, ApJ 536, 880.

Boden, A., Torres, G., & Hummel, C. 2005, ApJ 627, 464.

Carney, B., & Latham, D. 1987, AJ 92, 116.

Carney, B., Latham, D., Laird, J., & Aguilar, L. 1994, AJ 107, 2240.

Colavita, M. 1999, PASP, 111, 111.

Colavita, M. et al. 1999, ApJ, 510, 505.

Demarque, P., Woo, J.-H., Kin, Y.-C., & Yi, S., K. 2004, ApJS 155, 667.

Edvardsson, B. et al. 1993, A&A 275, 101.

ESA 1997, The Hipparcos and Tycho Catalogues, ESA SP-1200

Feltzing, S., Holmberg, J., & Hurley, J. 2001, A&A 377, 911.

Fouts, G. 1987. PASP99, 986.

Fuhrmann, K. 2002, NewA 7, 161.

Giclas, H., Burnham, R., & Thomas, N. 1971, Lowell Proper Motion Survey, Northern Hemisphere (Flagstaff: Lowell Observatory)

Giclas, H., Burnham, R., & Thomas, N. 1978, Lowell Obs. Bull. No. 164

Goldberg, D. et al. 2002, AJ124, 1132 (G2002).

Hummel, C. et al. 1998, AJ 116, 2536.

Johnson, D. & Soderblom, D. 1987, AJ 93, 864.

Latham, D. et al.1988, AJ, 96, 567.

Latham, D. et al. 2002, AJ, 124, 1144.

Luyten, W. 1979, 1980, "New Luyten Cataloge of Stars with Proper Motions Larger than Two Tenths of an Arcsecond" (Minneapolis: University of Minnesota Press).

Makarov, V. , Olling, R., & Teuben, P. 2004, MNRAS 352, 1199.

Mazeh, T. et al. 2003, ApJ 599, 1344.

Mermilliod, J.-C., & Mermilliod, M. 1994, Catalogue of Mean UBV Data on Stars, (New York: Springer)

Nordström, B. et al. 1994, A&A, 287, 338.

Nordström, B. et al. 2004, A&A 418, 989.

Pickles, A. 1998, PASP110, 863

Rocha-Pinto, H. et al. 2000, A&A 358, 850.

Rocha-Pinto, H. et al. 2004, A&A 423, 517.

Salim, S. & Gould, A. 2003, ApJ 582, 1011.

Skrutskie M. et al. 1997, in The Impact of Large Scale Near-IR Sky Surveys, eds. F. Garzon et al. (Dordrecht: Kluwer), 25.

Torres, G. et al. 2002, AJ 124, 1716 (Paper 1).

Venn, K. et al. 2004, AJ 128, 1177.

Wright, J., Marcy, G., Butler, P., & Vogt, S. 2004, ApJS 152, 261.

Yi, S. et al. 2001, ApJS 136, 417.

Yoss, K. 1961, ApJ 134, 809.

Zucker, S., & Mazeh, T. 1994, ApJ 420, 806.